CANDU MAINTENANCE CONFERENCE S08: INVESTIGATION AND REPAIR OF A CRACKED FEEDER AT POINT LEPREAU GS

by

A. Celovsky¹, M.D. Wright², T.S. Gendron², S.A. Usmani³, J. Slade⁴

ABSTRACT

Early in 1997 investigation of a low level leak in the Point Lepreau GS (PLGS) PHTS revealed that an outlet feeder, S08, was leaking. Ultrasonic inspection, and subsequent failure analysis, revealed that the leak was a consequence of a crack. Given the unusual nature of this event, and current concerns over feeder thinning, a detailed and careful removal and examination procedure was developed. The S08 outlet feeder was removed and shipped to Chalk River Laboratories for examination. The examination confirmed that the failure was a through-wall crack, most likely the consequence of stress corrosion cracking. A critical point of the analysis was to determine how the crack initiated, and subsequently propagated. High residual stresses and possibly abnormal loading in conjunction with chemistry environments resulted in the Stress Corrosion Cracking (SCC) of the S08 outlet feeder bend. It is recognized that some of the causative factors implicated in the S08 failure apply to other outlet feeders. In particular, residual stresses in the non-stress-relieved, short-radius cold bent pipes will remain relatively high over the future life of the feeders. However, the risk of CANDU feeder failure by SCC is judged to be extremely low based on the evidence of the inspections carried out to date and the good performance record of feeder pipe in the CANDU industry.

The channel was restored to its locked configuration, and the failed section of feeder replaced.

¹Reactor Materials Division

²Heat Exchanger Technology Branch
Chalk River Laboratories
Chalk River, Ontario K0J 1J0

³Process Engineering Branch, AECL, 2251 Spekman Drive, Mississauga, Ontario L5K 1B2

⁴Point Lepreau Generating Station P.O. Box 10 Point Lepreau, New Brunswick E0G 2H0

1. INTRODUCTION

The Point Lepreau Generating Station was shutdown on 17 January 1997, to investigate a low level primary heat transport heavy water leak. The leak was first detected on 1996 December 19 at a rate of approximately 1 kg/hour, and had increased to a rate of approximately 25 kg/hour by 1997 January 16.

A detailed search located the leak in the first bend of the outlet feeder pipe of fuel channel S08. In-situ radiography and ultrasonic inspections confirmed the leak was the result of a through-wall crack. The operating condition of the feeder pipe is summarized in Table 1.

To allow the reactor to be returned to service a program of repair and evaluation was initiated. This program included the following three major items:

- Removal, replacement of the cracked feeder pipe section and other feeder inspections.
- ii) Investigation of the cause of the crack.
- iii) Stress evaluation.

2. REMOVAL & REPLACEMENT; AND INSPECTION OF OTHER FEEDERS

2.1 Removal & Replacement

CANDU feeder pipes form a nested series of small diameter pipes either supplying or returning coolant to a fuel channel. Point Lepreau has 380 inlet and 380 outlet feeder pipes, arranged in an alternating supply and return configuration. Access of the fueling machine to the end of each fuel channel requires the feeder pipes to be connected at right angles to the fuel channel (see Figure 1). This compact core design, restricts access around the feeder pipes.

A three-dimensional CAD model of various options for feeder removal and replacement were studied. The restricted access and tight clearances precluded the use of both conventional automatic welding equipment and manual welding. Removing the feeder at the Grayloc hub, and at a some point downstream, minimized the number of field welds. Two options were pursued simultaneously:

- Development of a low clearance automatic welding machine, to allow welding just downstream of the crack.
- Removal of a longer section of feeder pipe, thereby allowing welding to take place further downstream at a less restricted area.

Channels S06, S07, and S08 were all de-fueled and S08 was isolated from the heat transport circuit using ice plugs. S07 and S08 were defueled in the event additional clearance requirements necessitated their removal. Even without removal of the S06 & S07 feeders, hydraulic jacking was required to spread the R08 and S08 endfittings. Prior to such a jacking operation, the maximum allowable jacking force was calculated to be 8 000 lbs. A jacking force of 5 000 lbs. was used and this spread the endfitting by 34 of an inch.

The low clearance automatic welding machine option resulted in some initial weld porosity. While the applicability of the first option was proven, available time in outage schedule made it possible to select the second option. The second option, which had the additional benefit of providing extra feeder pipe for detailed examination, was successfully used to install a replacement feeder section.

Welding was carried out in accordance with ASME Sec III class NB(1974) and AECL Technical Specifications. The resultant welds were inspected visually, radiographically, and using dye penetrant. Two sample welds were made and radiographically examined. A sample root pass weld was also made, immediately after the field welds, and visually examined.

2.2 Inspection of Other Feeders

To verify other feeders did not contain similar cracks, a UT inspection program on other feeders was conducted. Feeders similar to S08 were identified and then inspected. Similarities considered included, pipe diameter, bend radius, unlocked channel, and feeder spacer supports (see Section 4). A total of 157 feeders, comprising both inlets and outlets, were examined and no other crack-like indications were identified.

3. FAILURE INVESTIGATION

A series of tests and examinations were conducted on the failed feeder pipe elbow and on a spare elbow for comparison. The spare elbow was fabricated at the same time, using the same processes and from the same ingot material, as the failed elbow.

3.1 Visual Inspection & Sectioning

Other than the crack, a detailed visual inspection revealed no unusual features on either the OD or the ID surfaces of the pipe. No local pits, gouges, etc. were observed. The ID surface had fine surface features corresponding to local flow patterns, with some variation from the intrados to the extrados. Oxidation of the ID surface appeared uniform.

The pipe was sectioned as indicated in Figure 2, and further sectioned in and around the crack. Upon splitting the pipe into the E & F sections in Figure 2, it was noted that the pipe sprung open. This indicated high remaining residual stresses within the pipe. Increased hardness, within the bend section of pipe was also measured. Both the springing open of the pipe and the increased hardness was attributed to the cold bending process used during fabrication.

3.2 Gamma Spectral Analysis

A general radiation field of 190 μ Sv/hr was observed around the pipe. A gamma spectral analysis was conducted on the pipe and is summarized in Table 2. The types and quantities of radionuclides present are typical of a CANDU primary heat transport system. The radionuclides and quantities measured, are not known to cause stress corrosion cracking.

3.3 EC & UT Inspections

EC inspections conducted on the OD surface revealed only a single surface breaking defect. No other crack-like degradation was found elsewhere in the pipe. This defect was approximately 35 mm long at the OD. EC inspections were also conducted on the ID surface after the pipe section had been cut open. Again, only the single surface breaking defect

was revealed. The length of the flaw on the ID was approximately 63 mm long.

A limited series of UT wall thickness measurements were conducted on the failed pipe section and the spare elbow. Although the wall thickness of the failed component was thinner than the spare elbow, it was concluded that the difference was due to Flow Accelerated Corrosion, and was independent of the cracking mechanism. UT wall thickness measurements also indicated thinning of the pipe wall thickness along the pipe extrados and thickening of the wall thickness along the intrados. This was observed on both the spare elbow and the failed pipe section, and is consistent with the bending process used during fabrication.

3.4 Chemical Analysis

A full chemical analysis of the failed pipe material showed the material was in compliance to code of construction requirements, see Table 3 [1]. Numerous elemental spectra were also obtained using EDX, including spectra at the fracture surface. All elemental spectra obtained, indicated elements consistent with SA 106 Grade B pipe.

3.5 Residual Stress Measurements

Measurements of residual stress were made at positions through the wall thickness of the material on the spare elbow using a nondestructive neutron spectrometer. The residual stresses were measured on the spare elbow at a location equivalent to the crack on the failed component [1] (See Figure 3). The residual stress measurements showed that the hoop stress varied from compressive at the OD surface to tensile at the ID surface. The maximum tensile stress was 330 MPa, which approximates the yield point of the material of 350 MPa. Additional residual stress measurements were conducted after 20, 40, and 87.5 hour heat treatments at 308°C, the nominal temperature of the primary coolant. As expected, there was no apparent relaxation of the residual stresses at the nominal coolant operating temperature [2] (see Figure 3). Residual stresses were measured to be a maximum at the location equivalent to the crack defect [1].

From these measurements, it was concluded that the high residual stresses were present in the failed component during its in-service period. This is consistent with the observation that the pipe section sprung open during sectioning and the increased hardness in the bend region.

3.6 Metallurgical Examination

General Pipe Condition

Specimens were cut remote from the crack to determine the general morphology of the inside and outside surfaces as well as the deposit/oxide thickness. The inside surface of the pipe was scalloped around the entire circumference (Figures 4 and 5), with an oxide thickness of less than about 1 µm. In cross-section, the oxide was found to be ~1 µm thick, and exhibited a single-phase, compact structure typical of that expected for high flow outlet feeder conditions which can limit the oxide film thickness.

The outside surface was generally smoother than the inside, but with thick deposits. Inclusions in the feeder pipe material appeared to be consistent with the sulphur content (0.016 wt. %) and fabrication route of the pipe. When etched (Figure 6) the grain structure consisted of ferrite and pearlite grains, typical for SA 106B, with a decarburized zone of ~100 μm depth on the outside surface only. Vickers hardness measurements made remote from the crack gave an average value of 183 HV (20 kg). Immediately adjacent to the crack, the Vickers hardness values ranged from 203 to 223 HV (20 kg). Microstructure and hardness are consistent with a cold-bending process.

A section of the pipe to Grayloc hub weld region was prepared for examination of the heat-affected zones (HAZ) of the weld (Section A in Figure 2). No cracking, intergranular attack, or crack initiation was observed in the one plane of the HAZ examined.

Crack Examination

The upstream end of the crack, see Figure 5, was cut to enable metallographic cross-sections to be taken through the crack. Three cross-sections through the crack were examined. These cross-

sections showed not only the main crack and the branches observed on the inside surface of the pipe, but also numerous adjacent finer secondary cracks (Figure 7). All of the cracks showed micro-branching and followed an irregular path. Upon etching, the crack path was observed to be intergranular. There were very few transgranular fracture features. At high magnification, all the cracks were observed to be oxide-filled (Figure 8).

Two of the cross-sections were examined by electron microscopy, each showing identical features (Figure 9). Oxide was present in all cracks. The oxides in the wider cracks had the thickest oxide films (up to 10 µm) and exhibited a duplex structure, characteristic of a Potter-Mann type film [3] usually formed in low flow conditions. The oxide thickness could not be used to date the crack because the oxide growth is by both direct oxide formation and dissolution/re-precipitation. The rate of oxide growth by both mechanisms are affected to different degrees by different parameters and are not linear with time [4].

No evidence of inclusions, or other features, within the crack or crack tips was found.

Close to the ID surface, the fracture was eroded and the features reflected the banding of the underlying microstructure (Figure 10). The remainder of the fracture was generally covered with magnetite crystals; however, visible regions of the fracture appeared to be intergranular. After removal of the magnetite crystals, no additional features were detected, such as fatigue striations or beach marks. The fracture was observed to be mostly intergranular (Figure 11). Crack initiation appeared to occur at the inside surface of the pipe as evidenced by the crack shape. No obvious initiation site(s) was observed. The radial marks on the fracture surface suggest that crack growth was predominantly in the radial direction along the entire crack length. An estimate of the crack depth (a) to length (c) ratio was made using the crack profile. The estimated a/c was 0.25.

3.7 Cause of the Failure

NDE showed that the through-wall defect was a single crack with some secondary cracking,

without any other crack growth elsewhere on the pipe. There was nothing unusual in the microstructure or chemical composition of the pipe to suggest any undue susceptibility of this pipe to any cracking mechanism, with the possible exception of the increased hardness resulting from the cold bending process and the associated residual stress.

Scallop markings were observed on the inside surface of the feeder pipe consistent with corrosion in a high flow environment. However, there was no consistent correlation between the surface crack path and the scallop pattern indicating that they had played a role in crack initiation. The crack shape and general morphology were entirely consistent with initiation from the inside surface, but no pits, grooves, cavitation marks, foreign objects, or mechanical damage that could have acted as initiation sites were observed. However, if initiation occurred some time ago, the initiation site that may have been present could have been removed by the same corrosion process responsible for the scallop markings. The evidence for a loss in wall thickness is the lack of a decarburized zone at the ID as well as wall thickness measurement comparisons between the failed pipe section and the spare elbow. The wall thickness comparison suggests a loss in wall thickness of approximately 1 mm in 12.4 EFPY. Another feature that may be attributed to corrosion was the 0.7 mm deep open, river-like nature of the central region of the crack mouth.

The fracture surface away from the crack mouth. particularly remote from the through-wall portion, was not damaged by corrosion and therefore yielded evidence for the mechanism of fracture. The semi-elliptical shape of the fracture and the even, rounded crack front is consistent with fatigue crack propagation. However, other features which usually implicate fatigue such as beach marks and striations were absent. In addition, the presence of macroscopic features with relief on the order of 500 µm are atypical of fatigue. The strongest evidence against a fatigue cracking mechanism is the intergranular crack path, observed in all areas, including the tip of the growing crack. Thus, purely mechanical fatigue was not the cracking mechanism, even though cyclic stresses would have undoubtedly been present.

Some of the fracture features, for example the oxide-filled crack and the elliptical, even crack front, are characteristic of corrosion fatigue. However, the intergranular crack path is not characteristic and neither are the multiple crack paths (resulting from branching rather than multiple initiations). In addition, although corrosion fatigue is described as cracking, in most instances there is a noticeable metal loss from dissolution, creating parallel-sided, sometimes trench-like cracks. In the failed S08 feeder pipe, the opposite fracture faces mated very well which is inconsistent with corrosion fatigue.

The metallography and fractography showed no evidence for hydrogen embrittlement or brittle cleavage fracture, which sometimes have features in similar to with fatigue, and could have resulted in cracks superficially similar to this failure. There were no features observed to implicate creep in the failure, for example, grain boundary void formation. Finally, liquid or solid metal embrittlement, which can produce intergranular and branched crack paths, are not feasible since no embrittling species (e.g. Cu, Sb, Pb) were found within the cracks and none are expected in sufficient quantities in the steel or HTS.

The mechanism fitting the majority of the crack features discussed above, is stress corrosion cracking (SCC). The most distinctive of these is the intergranular and branched crack path. SCC can be driven by residual stress alone and evidence suggests the high residual stress at the crack location was a very significant factor in this failure. The crack was tightly closed and relatively difficult to see on the outside surface. This indicates the operating stresses were not high enough to cause general plastic rupture resulting in opening of the crack, even though the crack tips may have been propagating under high stress intensities during the final stages of crack growth. The low aspect ratio (a/c = 0.25) is also consistent with growth dominated by residual stresses.

Although SCC driven by residual stress is the most likely failure mechanism, it must be recognized that within the broad definition of environmental cracking, SCC and corrosion fatigue lie at two extremes of a continuum of degradation mechanisms depending on the relative contribution of cyclic stress and crack-tip strain-rate [5, 6]. Therefore, although it is

thought that the mechanism is best described as stress corrosion cracking, this does not rule out a contribution from cyclic stresses. In this respect, the very even crack front and the converging crack planes to give a single, relatively straight crack at the outside surface suggests a high stress dependence, possibly cyclic, which is not always necessary for SCC. In contrast, SCC more typically produces an uneven, jagged-shaped crack front and a tree-like cracking pattern.

SCC of carbon steel in the nuclear industry is a relatively rare event, requiring specific combinations of stress, temperature, and chemistry that deviate from normal operating conditions. The distribution of stresses resulting from the residual (Section 3.4), operating and dynamic stresses (Section 4, below), were evaluated. The applicable temperatures were available from the reactor operating history. The exact chemistry regime during all aspects of operation, especially transients, were more difficult to estimate. However, none of the classic environments that cause SCC of carbon steels should be operative under CANDU HTS conditions including excursion chemistries within the design envelope. One possible exception is carbonate contamination, which in alkaline aqueous solutions can cause intergranular SCC but concentrations required are relatively high, in the 1000 ppm range [7]. However, there are similarities between carbonate cracking and the observed crack. Thus, carbonate cracking is considered a plausible environment and potential sources of carbonate in the HTS are being reviewed. An additional environmentally-assisted cracking mechanism being considered is high temperature oxygen-assisted cracking [8]. While this mechanism does not normally result in intergranular cracks, threshold oxygen level could be reached during start-up and fueling transients [9]. The threshold oxygen levels are in the 5 and 50 ppb range. Susceptibility is greatest between 200°C and 250°C but failures have been reported at temperatures up to 320°C. The morphology of this type of cracking normally has features in common with corrosion fatigue and cracking is usually only seen when a dynamic load component is present. Despite the rare occurrence of intergranular cracking due to high temperature, oxygen assisted SCC, the fact that the necessary environmental conditions could be met during start-up or fueling means that this mechanism is also considered plausible, and is being investigated further.

Additional work is required to identify precisely the chemical environment responsible for the SCC and whether dynamic stress or residual stress alone was the dominant mechanical factor.

4. STRESS ANALYSIS

Loading of the failed S08 feeder pipe and the similar S15 feeder were evaluated to determine the stress distributions. A three-dimensional, finite element computer model was created using the ANSYS program. The model was developed using an 8-node brick element with three layers of elements through the pipe thickness (See Figure 12). The intrados and extrados pipe thickness was based on the UT wall thickness measurements. The model incorporated the residual stresses from the cold-bending operation, operating loads, static and dynamic loads, and loads from re-fuelling operations.

Using the model developed, various scenarios were evaluated. The principle configurations evaluated were:

- Atypical S08 feeder spacers resulting from the 2 ½ inch diameter feeder being adjacent to a larger diameter feeder (see Figure 1).
- The normal design configuration of a single end of the fuel channel locked in position.
- The abnormal situation were the S08 fuel channel was left unlocked after the 1995 Spacer Location and Re-positioning (SLAR) program.

The following significant results were obtained:

- For the normal design configuration of one end of the fuel channel locked and including the incorporation of the atypical feeder spacer assembly, the stresses in the S08 inlet and outlet feeders meet the requirements of the ASME code. Therefore, the atypical feeder spacer configuration of the outlet feeder S08 (and similarly the identical outlet feeder S15) were considered acceptable.
- The piping stresses in the unlocked S08 fuel channel in combination with the atypical feeder spacer results in considerably higher stresses in the outlet feeder compared to the inlet feeder.
- Without the imposition of the atypical S08 feeder spacer, the stresses in the feeder are

only marginally increased by a resultant 12.5 mm movement of the fuel channel arising from an unlocked condition. Only a marginal increase occurs because the feeder pipe assembly has sufficient flexibility to accommodate such movements.

 With the atypical S08 feeder spacer in combination with the unlocked fuel channel, a 12.5 mm channel movement during refueling increases the maximum stresses in the outlet feeder by 79% compared to the normal design configuration.

The additional stresses due to the combination of the unlocked channel, atypical feeder spacer, and normal fueling machine loads could result in a local dynamic strain in the crack region exceeding 0.3%. This level of strain is sufficient to initiate SCC, when the applied load produces strain rates in a critical range, and when appropriate environmental conditions exist.

5. SUMMARY

The successful removal and replacement of CANDU feeder pipes requires detailed planning due to the restricted access and tight clearances.

In-situ inspection of other inlet and outlet feeder pipes found no other crack-like defects.

Visual inspecton, NDE, and metallography revealed that the through-wall defect was a single crack with some secondary cracking, 35 mm long on the outside surface of the pipe and 63 mm long on the inside surface. No other crack-like degradation was found elsewhere in the pipe. The crack initiated at the inside surface of the pipe. No initiating feature was found but corrosion may have removed evidence of an initiation feature. Scallop markings were observed on the inside surface of the feeder pipe consistent with corrosion in a high flow environment. However, there was no indication that the scollop markings played a role in crack initiation.

The chemical composition and the microstructure of the pipe material was typical of SA 106 Grade B pipe. The pipe elbow at the crack defect area had increased hardness and high residual stresses attributed to the cold bending process used during fabrication.

The physical features of the crack are typical of stress corrosion cracking (SCC), although a cyclic load may have contributed to the failure. Additional work is required to identify precisely the chemical environment responsible for the SCC.

The CANDU core design must support and restrain the core, fuel channels, and feeder piping while providing flexibility to accommodate thermal expansion and dynamic loadings from such items as the fueling machine. The Point Lepreau pipe restraint system indicated the S08 channel and feeder were not returned to the original design configuration after the 1995 SLAR operation. This resulted in additional dynamic loadings in the S08 outlet feeder during re-fueling operations. Furthermore, the configuration of the unlocked S08 channel in combination with its atypical feeder spacer system resulted in loading conditions where SCC could occur in the outlet feeder

8. ACKNOWLEDGEMENTS

The authors wish to acknowledge the many people at NBP, Ontario Hydro, and AECL who contributed to conducting this work on a priority basis. Special thanks are extended to Doug Rogers, Steve Bushby, Doug Miller, and Malcolm Clarke, who were instrumental in completing this work.

9. REFERENCES

- A. Celovsky, A. and Root, J.H., "Measurements on Point Lepreau S08 Feeder Pipe and Spare Elbow," AECL Report RM-RP-22, 1997 May (Draft)
- Price, E.G., "Stress Relaxation Creep and Tensile Test on A106B Feeder Pipe Material" AECL Report IR 453, 1982.
- 3. Potter, E.C. and Mann, G.M.W, "Oxidation of Mild Steel in High-Temperature Aqueous Systems", 1st Intl. Congress on Metallic Corrosion, London, 417-426, 1962.

- Moore, J.B., and Jones, R.L., "Growth Characteristics of Iron Oxide Films Generated in Dilute Lithium Hydroxide Solution at 300°C", J. Electrochemical Soc., 115:576-583, 1968.
- Andresen, P.L. and Ford, F.P., "Life Prediction by Mechanistic Modeling and System Monitoring of Environmental Cracking of Iron and Nickel Alloys in Aqueous Systems" Mat. Sci. and Eng. A103, 161-181,1988.
- 6. Parkins, R.N., "Strain Rate Effects in Stress Corrosion Cracking" Corrosion 46, 178-189, 1990.

- Kmetz J. H. and Truax D. J., "Carbonate Stress Corrosion Cracking of Carbon Steel in Refinery FCC Main Fractionator Overhead Systems" CORROSION 90, paper 206, Houston TX, NACE 1990.
- Scott, P.M. and Tice, D.R., "Stress Corrosion in Low Alloy Steels" Nuclear Engineering and Design 119, 399-413, 1990.
- Elliot, A.J., "Review of HTS Chemistry Related to Possible Crack Initiation in Carbon Steel" AECL Memorandum to T. Gendron and M. Wright, 1997 January 31 (Draft).

TABLE 1: AVERAGE S08 OUTLET FEEDER OPERATING CONDITIONS

Operating Conditions	Lifetime Averaged Value for S08 Outlet Feeder	
Years In-Service	12.4 EFPYs	
Temperature	310.9 °C	
Quality	0.82 %	
Mass Flow	24.4 kg/s	
Flow Velocity	15.7 m/s	
Time in Boiling	37.8 %	

TABLE 2: RADIONUCLIDE INVENTORY OF REMOVED PIPE SECTION

ISOTOPE	QUANITY (Bq)
Cr-51	1.58 x 10 ⁵
Mn-54	2.66 x 10 ⁴
Fe-59	2.73 x 10 ⁵
Co-58	7.91×10^3
Co-60	1.49×10^3
Zr-95	1.22 x 10 ⁶
Nb-95	2.82×10^6
Ru-103	1.46 x 10 ⁵
Sn-113	1.42×10^4
Sb-122	4.79×10^4
Sb-124	3.49×10^5
I-133	4.06 x 10 ⁴
La-140	3.35×10^4
Ce-141	7.99 x 10 ⁴
Ce-144	5.30 x 10 ⁴
Hf-181	2.44 x 10 ⁴

TABLE 3: CHEMICAL ANALYSIS RESULTS ON FEEDER PIPE MATERIAL

Concentrations in Wt. %				
Element	SA 106 Grade B (1977 Ed.)	S08 Pipe Mill Cert. (1975)	S08 Pipe (Measured in 1997)	
С	0.30 max.	0.19	0.161 ±0.008	
S	0.058 max.	0.011	0.0160 ±0.0015	
P	0.048 max.	0.022	0.0165 ±0.0020	
Mn	0.29 to 1.06	0.65	0.62 ±0.02	
Ni	*	0.020	0.0137 ±0.0006	
Cr	*	0.030	0.0236 ±0.0009	
Mo	NS		< 0.0015	
V	NS		0.0041 ±0.0005	
Cu	*	0.013	0.0119 ±0.0005	
Si	0.10 min.	0.33	0.295 ±0.015	
Co	0.0060*	0.0039	-	

NS Not Specified

^{*} Not specified for 1977 Edition of SA 106 material, but additional requirement imposed by AECL Technical Specification.

FIGURE 1: S08 FEEDER ARRANGEMENT

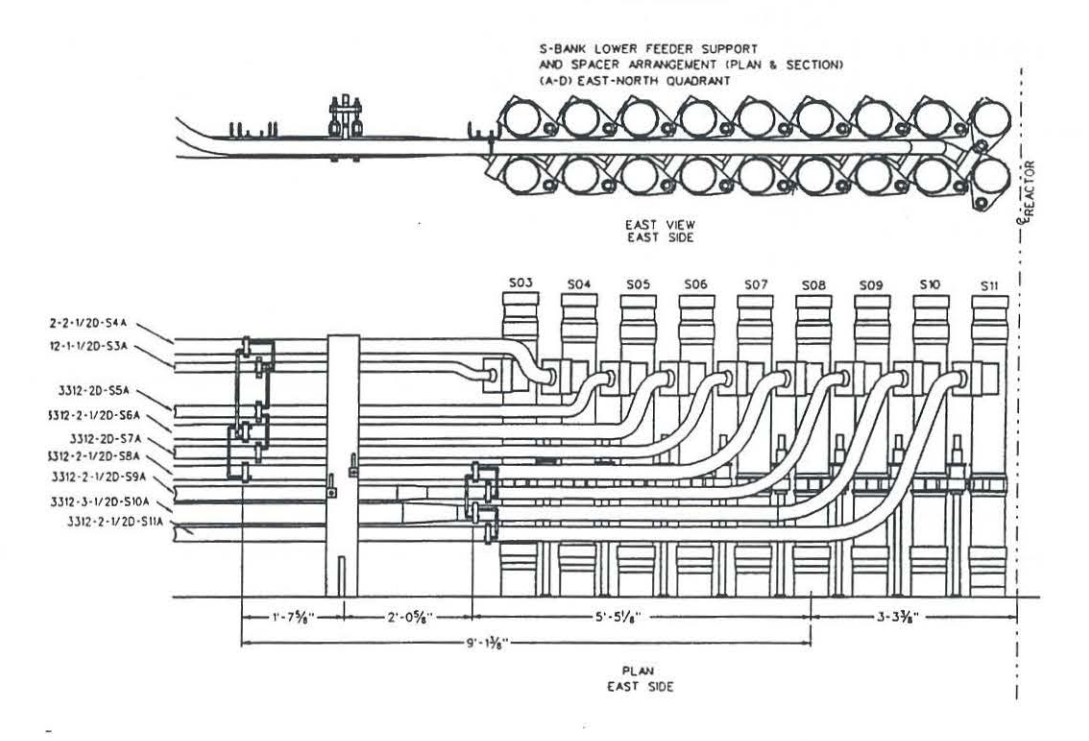


FIGURE 2: SECTIONING DIAGRAM OF S08 PIPE SECTION

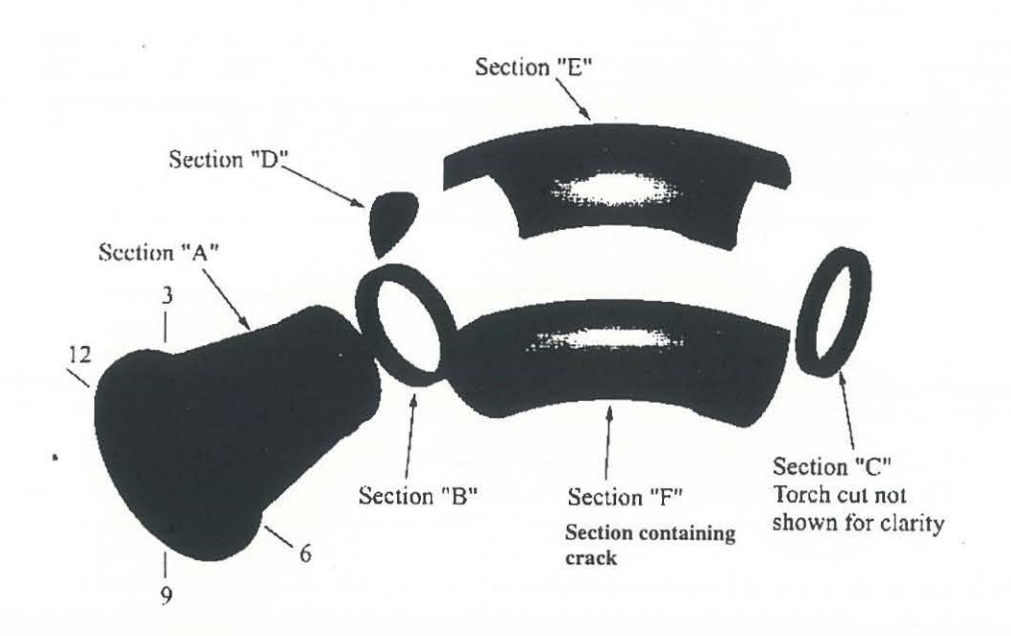


FIGURE 3: RESIDUAL STRESS SCANS OF ARCHIVED ELBOW

400 Stress (MPa)

200

-200

-200

-400

-600

Distance from Outer Surface (mm)

O As received

□308 C, 20 h △308 C, 40 h ※308 C, 87.5 h

2 3 4 5 6 7

FIGURE 4: SEM, SECONDARY ELECTRON IMAGE, OF AREA REMOTE FROM THE CRACK SHOWING SCOLLOPS

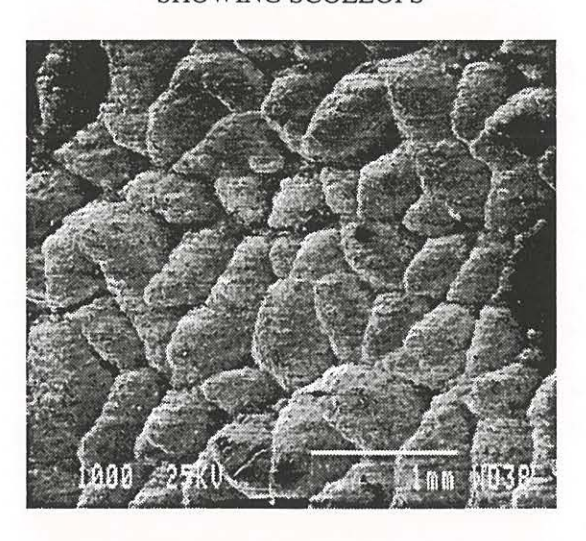


FIGURE 5: PHOTOGRAPH OF THE MONTAGE ASSEMBLED FROM SEM, SECONDARY ELECTRON IMAGES, OF THE ENTIRE CRACK LENGTH (ID SURFACE)

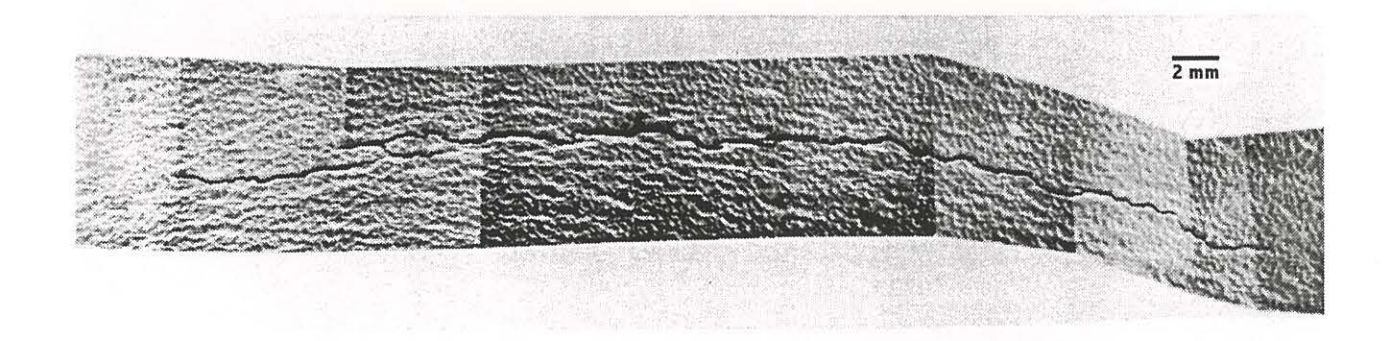


FIGURE 6:
MICROSTRUCTURE OF FEEDER PIPE
CIRCUMFERENTIALLY ADJACENT TO
THE CRACK SHOWING BANDED
FERRITE/PEARLITE GRAINS

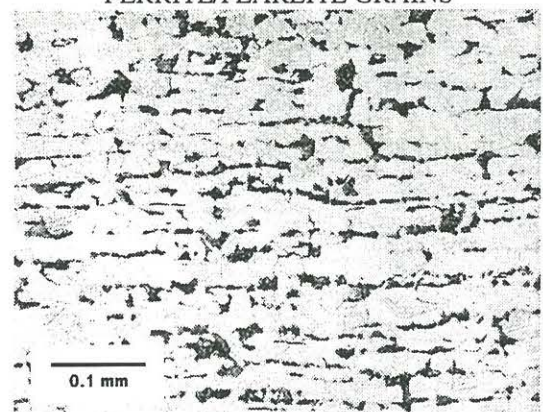


FIGURE 7: INTREGRANULAR CRACK IN FEEDER PIPE (ETCHED, RADIAL-CIRCUMFERENTIAL PLANE)

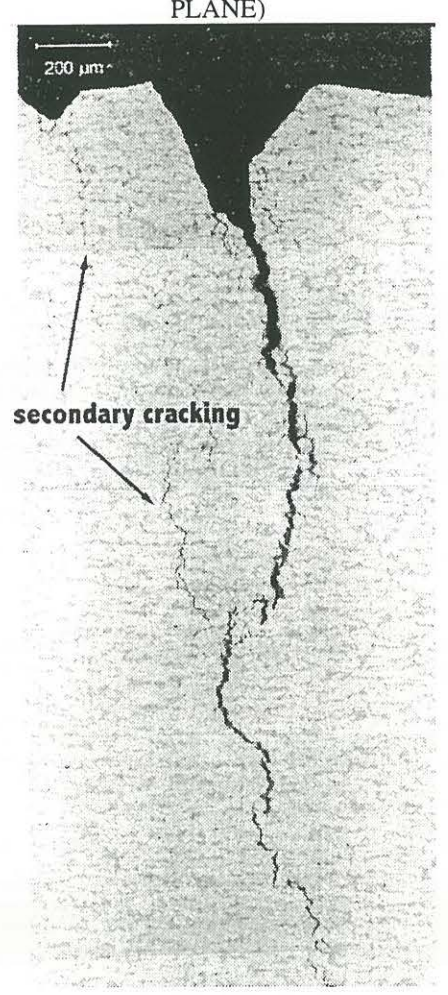


FIGURE 8:
OXIDE FILLED INTRAGRANULAR CRACK
IN FEEDER PIPE (RADIALCIRCUMFERENTIAL PLANE)

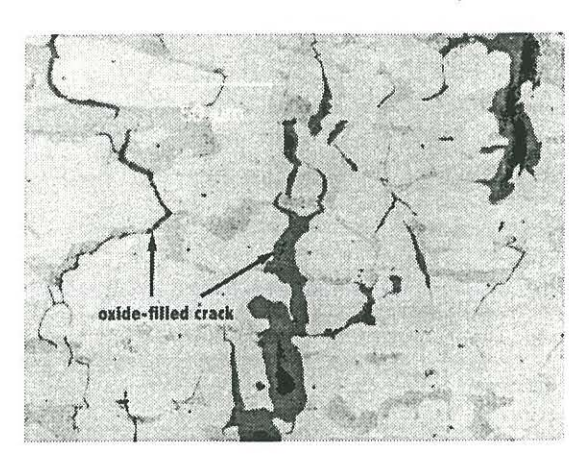


FIGURE 9: SEM, SECONDARY ELECTRON IMAGE, OF CRACK ON CROSS SECTION

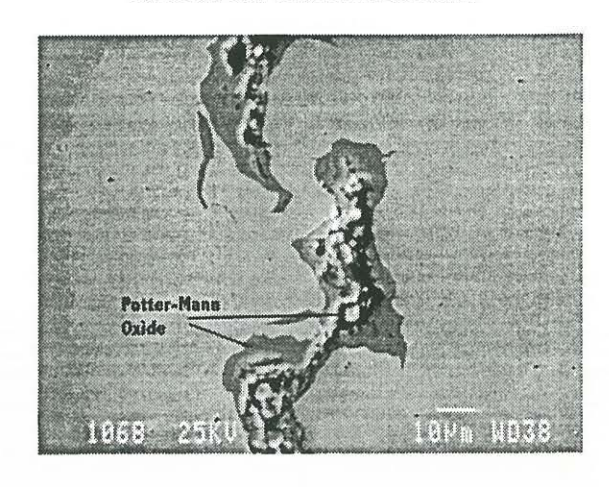


FIGURE 10: SEM, SECONDARY ELECTRON IMAGE, OF FRACTURE SURFACE SHOWING ERODED REGION AT INSIDE SURFACE OF THE PIPE AND DEPOSITS ON FRACTURE

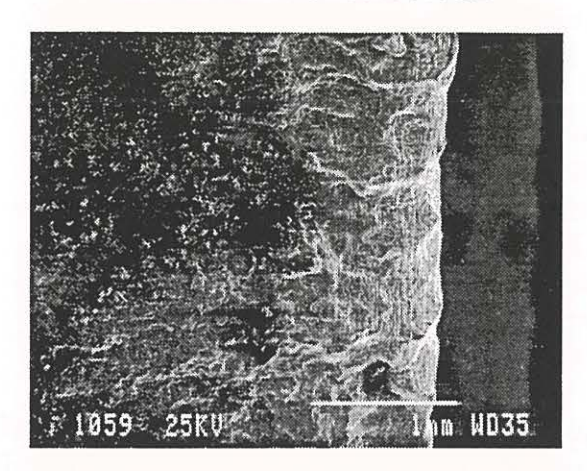


FIGURE 11:
SEM, SECONDARY ELECTRON IMAGE, OF
FRACTURE SURFACE AFTER CLEANING
TO REMOVE SURFACE DEPOSITS
SHOWINGS PREDOMINANCE OF
INTERGRANULAR FRACTURE

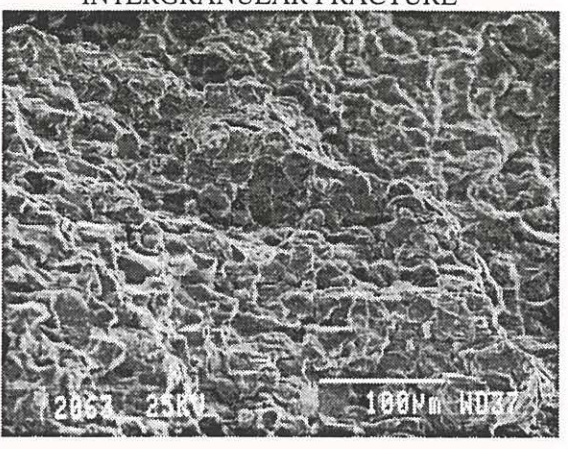


FIGURE 12: FINITE ELEMENT MODEL OF S08 ELBOW INCREASING STRESS LEVELS FROM A THROUGH I

